Journal of Physics and Chemistry of Solids ▮ (▮▮▮▮) ▮▮▮–▮▮▮

Contents lists available at SciVerse ScienceDirect

Journal of Physics and Chemistry of Solids

journal homepage: www.elsevier.com/locate/jpcs

Beat excitation of terahertz radiation in a semiconductor slab in a magnetic field

Manish Kumar [a,*], Lalita Bhasin [b], V.K. Tripathi [b]

[a] Department of Electrical Engineering, I.T., B.H.U., Varanasi-221005, India
[b] Physics Department, Indian Institute of Technology, Delhi, India

ARTICLE INFO

Article history:
Received 3 November 2010
Received in revised form
21 September 2011
Accepted 24 October 2011

Keywords:
A. Semiconductors

ABSTRACT

Two infrared lasers of frequencies ω_1 and ω_2 propagating in the TM/TE mode along $\hat{z}$ direction in a rippled density semiconductor waveguide are shown to resonantly excite terahertz radiation at the beat frequency when ripple wave number is suitably chosen to satisfy the phase matching. The wave vector of the density ripple is along the direction of laser propagation while a static magnetic field is applied transverse to it. The lasers exert a ponderomotive force on the electrons at the beat frequency. This force, in the presence of density ripple and transverse magnetic field, produces a nonlinear current at the terahertz frequency. The magnetic field enhances the amplitude of the terahertz wave. However terahertz yield is significantly higher in the TM mode laser beating than in the TE mode laser beating.

1. Introduction

The generation of terahertz (THz) radiation has attracted attention of many researchers worldwide in recent years. These waves, ranging from 0.1 to 50 THz, have found widespread applications in the field of biological imaging[1], remote sensing[2], spectroscopy of solids and liquids[3], chemical and security identification[4], etc. One may generate THz radiation by the following optical methods: (i) optical rectification, (ii) difference frequency generation (DFG), (iii) parametric generation. These are basically second order nonlinear processes and occur in non-centrosymmetric materials. In the optical rectification process, one requires a fs laser pulse. The electric field of the THz pulses may be calculated from the wave equation by including a nonlinear current source. The basic limitation of this process is difficult phase matching and limited output power. Only in specific spectral range of pump pulse and generated THz wave, the phase matching can be achieved. Another obvious disadvantage is broad line width, which is proportional to τ_L^{-1} where τ_L is the pulse duration[5]. THz generation by DFG and parametric oscillation is possible with ns laser pulses or cw lasers. Continuously tunable and coherent radiation in the wide spectral range has been achieved[6–8]. In the DFG, two collinear phase matched laser beams are required. The process has high conversion efficiency, which leads to high output power. CW THz waves thus obtained have narrow linewidths[9]. THz wave parametric oscillators are based on stimulated scattering in crystals such as $LiNbO_3$. The advantages of this method include continuous tunability, design simplicity and room temperature operation. However one obtains limited output power due to phase mismatch[10].

THz emissions have also been produced from plasmas using energetic electron beams and subpicosecond laser pulses. These include coherent radiation from plasma oscillations driven by ultrashort laser pulses [11], transition radiation of electron beams [12], synchrotron radiation from accelerator electrons [13], Cherenkov wake radiation in magnetized plasmas [14]. Earlier Hamster et al. [11] observed high power terahertz radiation from short pulse laser produced plasma, employing 1TW, 100 fs laser focused onto gas and solid targets. Recently, Antonsen et al. [15] proposed a scheme of ponderomotive force induced resonant terahertz generation in a rippled density plasma. The terahertz power scales as the square of laser intensity. Bhasin et al. [16] introduced a scheme of resonant terahertz radiation generation by the optical rectification of a picosecond laser pulse in a rippled density magnetized plasma . The terahertz power scales as the square of density ripple amplitude and rises with the magnetic field strength. Kumar et al. [17] have investigated the beat excitation of THz radiation using Gaussian laser beams co-propagating along the direction of ambient magnetic field in a rippled density plasma channel. The density ripple provides phase synchronism while the axial magnetic field enhances the nonlinear coupling through cyclotron resonance.

Tunable terahertz radiation generated in semiconductors by an ultrashort light pulse is known to be due to coherent effects in the photogenerated plasma during optical excitation in the surface depletion region or in the electric field region of a biased semiconductor. Hashimshony et al. [18] reported tunable radiation in the

* Corresponding author. Tel.: +91 542 2570619 (Home), +91 8853951326 (Mobile).
E-mail address: kumarmanish21@hotmail.com (M. Kumar).

0022-3697/$ - see front matter © 2011 Elsevier Ltd. All rights reserved.
doi:10.1016/j.jpcs.2011.10.031

range of 0.1 to a few THz by the interaction of a superluminous photoconducting front with an electrostatic frozen wave configuration. Glinka et al. [19] have reported the generation of THz oscillation by a femtosecond optical pulse in the μm-sized LT–GaAs slab grown on the GaAs substrate. McLaughlin et al. [20] have reported substantial enhancement in TE mode in the presence of magnetic field in InAs. The conversion efficiency continues to rise with an increasing magnetic field up to 8 T. Such enhancement of the visible to THz conversion efficiency is extremely beneficial for potential applications of THz radiation such as imaging [21]. Furthermore, recent studies [22–24] have demonstrated that increased THz powers may be achieved at low magnetic fields, $B=1.7$ T. Heyman et al. [25] studied terahertz emission from InAs and GaAs in a magnetic field and observed ultrashort THz pulses. They observed 12 μW average terahertz power from n–InAs at $B=3.2$ T. In a separate but related study, Shulman et al., have carried out experimental work on n–GaAs/Al tunnel junctions and found an effective enhancement of the radiation intensity close to semiconductor–metal interface [27].

In this paper we study beat excitation of THz radiation by TM/TE mode lasers propagating through a rippled semiconductor slab while there exists a static magnetic field is transverse to the direction of laser propagation. Our calculations are based on two semiconductors viz., Ge ($\varepsilon_L=14$) and GaAs ($\varepsilon_L=17$). The wave vector of the density ripple is along the direction of laser propagation. Two laser pulses, co-propagating in the semiconductor, exert a ponderomotive force on the electrons at the beat frequency and beat wave vector. This force, in the presence of density ripple and transverse magnetic field, produces a nonlinear current at the terahertz frequency. The density ripple wave number provides the requisite phase matching. In Section 2 we study laser propagation in the semiconductor slab and obtain the dispersion relation. In Section 3 we examine the nonlinear process of beat excitation of terahertz wave. In Section 4 we derive the dispersion relation for the THz radiation. In Section 5, a brief discussion of results is given.

2. Laser propagation through a semiconductor slab

Consider a semiconductor slab of thickness 2a, where origin passes through the center of the slab as shown in Fig. 1. Two TM mode lasers propagate through it in the $\hat{z}$ direction. A static magnetic field $\vec{B}_s$ is also applied in the $\hat{y}$ direction. The variation along y-direction is assumed to be zero i.e. $\partial/\partial y=0$. The electric fields of the two lasers are

$$\vec{E}_j=\vec{A}_{j0}(x)e^{-i(\omega_j t-k_{zj}z)},\ j=1,2 \tag{1}$$

From third and fourth Maxwell's equations viz.

$$\nabla\times\vec{E}=-\frac{1}{c}\frac{\partial\vec{B}}{\partial t},\quad \nabla\times\vec{B}=\frac{4\pi}{c}\vec{J}+\frac{1}{c}\frac{\partial}{\partial t}(\underline{\underline{\varepsilon}}\cdot\vec{E}),$$

in the limit $\vec{J}=0$ the wave equation turns out to be

$$\nabla^2\vec{E}_j-\nabla(\nabla.\vec{E}_j)+\frac{\omega_j^2}{c^2}(\underline{\underline{\varepsilon}}_j\cdot\vec{E}_j)=0 \tag{2}$$

where $\underline{\underline{\varepsilon}}_j$ is the permittivity tensor with components (cf. Appendix A):

$$\varepsilon_{jxx}=\varepsilon_{jzz}=\varepsilon_L-\frac{\omega_p^2}{\omega_j^2-\omega_c^2},\quad \varepsilon_{jyy}=\varepsilon_L-\frac{\omega_p^2}{\omega_j^2},\quad \varepsilon_{jxz}=-\varepsilon_{jzx}=-i\frac{\omega_c}{\omega_j}\frac{\omega_p^2}{\omega_j^2-\omega_c^2},$$

$$\varepsilon_{xy}=\varepsilon_{yx}=\varepsilon_{yz}=\varepsilon_{zy}=0,\quad \omega_c=\frac{eB_s}{mc},$$

is the electron cyclotron frequency, $\omega_{po}=\sqrt{(4\pi n_0e^2/m)}$ is the electron plasma frequency. $-$e and m are the electron charge and mass, respectively, n_0 is the equilibrium electron density in the slab and ε_L is the lattice permittivity of the semiconductor. For ω_1, $\omega_2\gg\omega_c$, the permittivity tensor turns out to be $\underline{\underline{\varepsilon}}_j=\varepsilon_j\,\underline{\underline{I}}$ where $\varepsilon_j=\varepsilon_L-\omega_p^2/\omega_j^2$. In this case the z-component of wave equation in region I can be written as

$$\frac{\partial^2E_{jz}}{\partial x^2}+k_{jx}^2E_{jz}=0,\quad (-a<x<a) \tag{3}$$

where $k_{jx}^2=(\omega_j^2/c^2)\varepsilon_j-k_{jz}^2$. The solution of Eq. (3) is given by

$$E_{jz}=A_I\cos k_{jx}x\quad\text{(For symmetric mode)} \tag{4}$$

In region II, the z-component of the wave equation can be written as

$$\frac{\partial^2E_{jz}}{\partial x^2}-\alpha_{jII}^2E_{jz}=0,\quad (|x|>a) \tag{5}$$

where $\alpha_{jII}^2=k_{jz}^2-\omega_j^2/c^2$. The solution of Eq. (5) is given by

$$\begin{aligned}E_{jz}&=A_{II}e^{-\alpha_{jII}x}\quad x>a\\&=A_{II}e^{\alpha_{jII}x}\quad x<-a\end{aligned} \tag{6}$$

The x-component of electric fields in regions I and II can be obtained by assuming $\nabla\cdot\vec{E}=0$. It gives

$$E_{jx}=-\frac{ik_{jz}}{k_{jx}}A_I\sin k_{jx}x\quad -a<x<a \tag{7}$$

$$E_{jx}=\frac{ik_{jz}}{\alpha_{jII}}A_I\cos k_{jx}a e^{-\alpha_{jII}(x-a)}\quad x>a \tag{8}$$

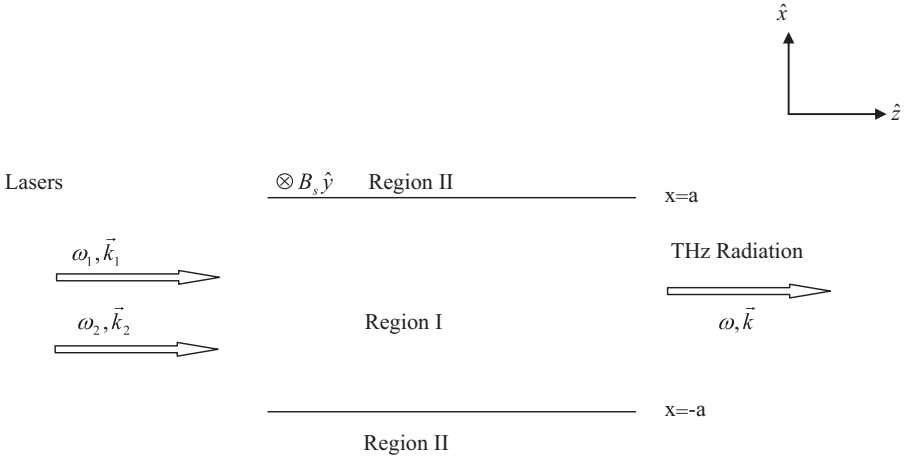

Fig. 1. System configuration.

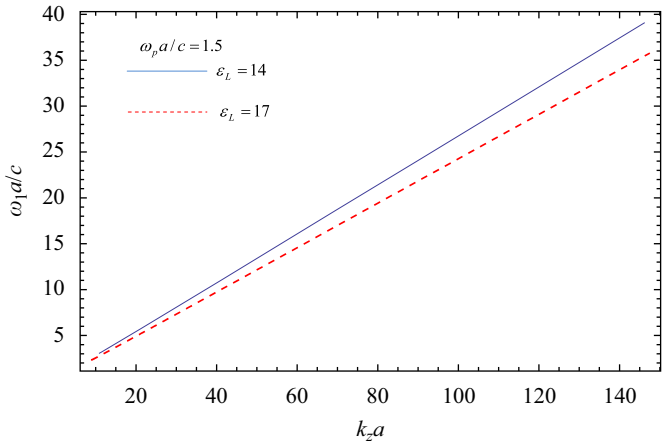

Fig. 2. Dispersion relation for TM_{10} mode.

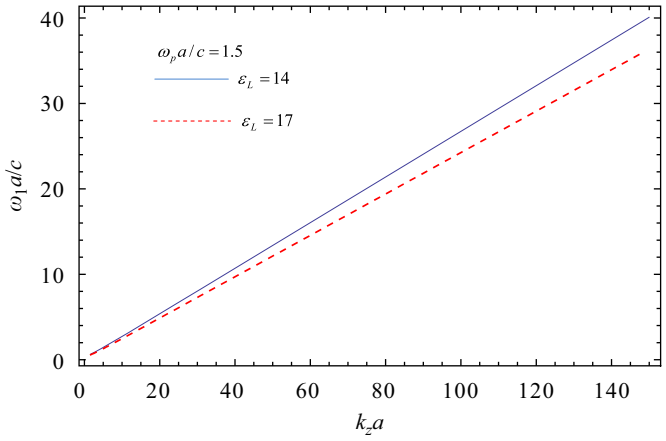

Fig. 3. Dispersion relation for TE_{10} mode.

Applying the boundary condition $E_{jx}^{I} = E_{jx}^{II}$ at $x=a$, the dispersion relation for TM_{10} mode laser is

$$\tan k_{jx} a = -\frac{k_{jx}}{\alpha_{jII}\varepsilon_j} \tag{9}$$

By a similar analysis, the dispersion relation for TE_{10} mode laser is

$$\tan k_{jx} a = \frac{\alpha_{jII}}{k_{jx}} \tag{10}$$

where for TE_{10} mode $k_{jx} = ((\omega_j^2/c^2)\varepsilon_j - k_{jz}^2)^{1/2}$. In Figs. 2 and 3, we plot dispersion relation for TM_{10} mode and TE_{10} mode, respectively. For $\varepsilon_L = 14$(Ge), 17(GaAs), $\omega_p a/c = 1.5$, $k_z a$ increases linearly as $\omega_1 a/c$ varies in the range 5–40 for both the modes. Also it shows that both the modes are guided in the semiconductor.

3. Beat excitation of terahertz nonlinear current density in magnetic field

Consider the propagation of two TM_{10} mode laser beams of frequencies ω_1, ω_2 and wave vector $\vec{k}_{1z}, \vec{k}_{2z}$, respectively inside the rippled semiconductor slab($n = n_{q0} e_{iqz}$, where q is the ripple wave vector), whose x and z components of electric fields are given by

$$E_{jz} = A_j \cos k_{jx} x e^{-i(\omega_j t - k_{jz} z)}$$
$$E_{jx} = A_j i \frac{k_{jz}}{k_{jx}} \sin k_{jx} x e^{-i(\omega_j t - k_{jz} z)} \tag{11}$$

where $k_{jx}^2 = (\omega_j^2/c^2)((\varepsilon_{jxx}^2 + \varepsilon_{jxy}^2)/(\varepsilon_{jxx})) - k_{jz}^2$ and $j = 1.2$. Similarly, for two TE_{10} mode laser beams the transverse electric field inside the semiconductor slab can be written as

$$E_{jy} = A_j \cos k_{jx} x e^{-i(\omega t - k_{jz} z)} \tag{12}$$

where $k_{jx} = ((\omega_j^2/c^2)\varepsilon_{jyy} - k_{jz}^2)^{1/2}$. These exert a ponderomotive force on the electrons given by

$$\vec{F}_p = -\frac{e^2}{2m\omega_1\omega_2} \nabla(\vec{E}_1 \cdot \vec{E}_2^*) \tag{13}$$

The nonlinear velocity response due to ponderomotive force is governed by the equation of motion

$$\frac{\partial \vec{v}_\omega^{NL}}{\partial t} = \frac{\vec{F}_p}{m} - \vec{v}_\omega^{NL} \times \vec{\omega}_c \tag{14}$$

where $\omega = \omega_1 - \omega_2$ and $k_z = k_{1z} - k_{2z}$. The x and z components of Eq. (15) can be written as

$$v_{\omega x}^{NL} = \frac{1}{m(\omega^2 - \omega_c^2)} [i\omega F_{px} - \omega_c F_{pz}], \tag{15}$$

$$v_{\omega z}^{NL} = \frac{1}{m(\omega^2 - \omega_c^2)} [\omega_c F_{px} + i\omega F_{pz}], \tag{16}$$

where F_{px} and F_{pz} are the x and z component of ponderomotive force, respectively. The nonlinear current at $\omega, \vec{k} + \vec{q}$ in the presence of density ripple $n_{q0} e^{iqz}$ can be written as

$$\vec{J}^{NL} = -\frac{1}{2} n_{q0} e \vec{v}_\omega^{NL} e^{iqz} \tag{17}$$

4. Dispersion relation for the terahertz wave

The wave equation for the THz wave can be written as

$$-\nabla^2 \vec{E} + \nabla(\nabla \cdot \vec{E}) = \frac{4\pi i\omega}{c^2} \vec{J}^{NL} + \frac{\omega^2}{c^2} (\underline{\underline{\varepsilon}} \cdot \vec{E}) \tag{18}$$

From the x-component of wave equation, neglecting the current source term, one obtains

$$E_x = -\frac{((\omega^2/c^2)\varepsilon_{xz} - ik_z(\partial/\partial x))}{((\omega^2/c^2)\varepsilon_{xx} - k_z^2)} E_z \tag{19}$$

Substituting this into the z-component of wave equation, replacing $k_z -> k_z - i\partial/\partial z$, one obtains

$$\frac{\partial^2}{\partial x^2} E_z + k_x^2 E_z + 2ik_z \frac{\partial}{\partial z} E_z = \frac{4\pi i}{\omega\varepsilon_{xx}} \left(\frac{\omega^2}{c^2} \varepsilon_{xx} - k_z^2 \right) J_z^{NL} \tag{20}$$

where $k_x = ((\omega^2/c^2)(\varepsilon_{xx}^2 + \varepsilon_{xz}^2)/\varepsilon_{xx} - k_z^2)^{1/2}$

In order to deduce the mode structure of the THz wave in the semiconductor, we neglect the current source and the last term on LHS, so Eq. (21) reduces to

$$\frac{\partial^2}{\partial x^2} E_z + k_x^2 E_z = 0, \tag{21}$$

whose solution is given by

$$E_z = A_3 \cos k_x x \quad -a < x < a$$
$$= A_3' e^{-\beta x} \quad x > a$$
$$= A_3' e^{\beta x} \quad x < -a \tag{22}$$

where, $\beta = (k_z^2 - \omega^2/c^2)^{1/2}$, $A_3' = A_3 \cos k_x a e^{\beta a}$. Applying the boundary conditions viz.

$$E_z^I = E_z^{II}, \quad x = \pm a$$
$$D_x^I = D_x^{II}, \quad x = \pm a$$

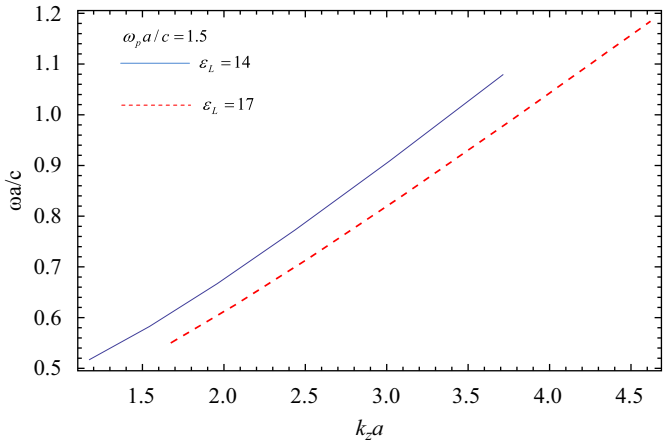

Fig. 4. Dispersion relation for Terahertz radiation in TM_{10} mode.

One obtains a dispersion relation

$$\tan k_x a - i\frac{\varepsilon_{xz}k_z}{\varepsilon_{xx}k_x} = \frac{1}{\beta k_x \varepsilon_{xx}}\left(\frac{\omega^2}{c^2}\frac{\varepsilon_{xz}^2}{\varepsilon_{xx}} - k_x^2\right) \tag{23}$$

In Fig. 4 we plot the dispersion relation for terahertz wave in TM_{10} mode. From figure we see that for $\varepsilon_L = 14$ and for $\varepsilon_L = 17$ the normalized terahertz frequency $\omega a/c$ increases linearly with normalized axial propagation constant $k_z a$ indicating terahertz wave in TM_{10} mode is guided in the semiconductor slab.

So when current source is included in the wave equation, the solution of wave is modified as

$$E_z = A_3(z)\psi(x)e^{-i(\omega t - k_z z)} \tag{24}$$

where

$$\psi(x) = \cos k_x x \quad -a < x < a$$
$$= \cos k_x a e^{-\beta(x-a)} \quad |x| > a$$

Substituting Eq. (25) in Eq. (21), one obtains

$$2ik_z\psi(x)\frac{\partial A_3}{\partial z} + A_3\left[\frac{\partial^2\psi(x)}{\partial x^2} + k_x^2\psi(x)\right] = R_z \tag{25}$$

where

$$R_z = -\frac{4\pi i}{\omega\varepsilon_{xx}}\left(\frac{\omega^2}{c^2}\varepsilon_{xx} - k_z^2\right)J_z^{NL} \quad -a < x < a$$
$$= 0 \quad |x| > a$$

At phase matching the last term on LHS cancel each other, multiplying Eq. (26) by $\psi^*(x)dx$ and integrating from $-\infty$ to $+\infty$ w.r.t. x and then integrating w.r.t z and normalizing, one obtains

$$\frac{A_3}{A_1} = \frac{1}{16}\left(\frac{n_q}{n_0}\right)\left(\frac{\omega_p^3}{\omega_1\omega_2(\omega^2-\omega_c^2)}\right)\left(\frac{\omega^2 - k_z^2/\varepsilon_{xx}}{k_z+q}\right)$$
$$\times\left(\frac{eA_2^*}{m\omega_p c}\right)\left(\frac{2k_x}{2k_x+\sin 2k_x}\right)R \tag{26}$$

where all quantities are normalized w.r.t. a and c. For TM_{10} mode laser beating

$$R = \begin{pmatrix} \frac{\sin(k_x-k_{1x}-k_{2x})}{k_x-k_{1x}-k_{2x}} + \frac{\sin(k_x+k_{1x}-k_{2x})}{k_x+k_{1x}-k_{2x}} \\ + \frac{\sin(k_x-k_{1x}+k_{2x})}{k_x-k_{1x}+k_{2x}} + \frac{\sin(k_x+k_{1x}+k_{2x})}{k_x+k_{1x}+k_{2x}} \end{pmatrix}$$
$$+\left(\frac{k_{1z}k_{2z}}{k_{1x}k_{2x}}\right)\begin{pmatrix} -\frac{\sin(k_x-k_{1x}-k_{2x})}{k_x-k_{1x}-k_{2x}} + \frac{\sin(k_x+k_{1x}-k_{2x})}{k_x+k_{1x}-k_{2x}} \\ + \frac{\sin(k_x-k_{1x}+k_{2x})}{k_x-k_{1x}+k_{2x}} - \frac{\sin(k_x+k_{1x}+k_{2x})}{k_x+k_{1x}+k_{2x}} \end{pmatrix}$$

and for TE_{10} mode laser beating

$$R = \begin{pmatrix} \frac{\sin(k_x-k_{1x}-k_{2x})}{k_x-k_{1x}-k_{2x}} + \frac{\sin(k_x+k_{1x}-k_{2x})}{k_x+k_{1x}-k_{2x}} \\ + \frac{\sin(k_x-k_{1x}+k_{2x})}{k_x-k_{1x}+k_{2x}} + \frac{\sin(k_x+k_{1x}+k_{2x})}{k_x+k_{1x}+k_{2x}} \end{pmatrix}$$

The phase matching criteria is

$$q = k_{1z} - k_{2z} - k_z \tag{27}$$

In Figs. 5 and 6, we plot normalized terahertz amplitude vs normalized terahertz frequency for TM_{10} and TE_{10} mode laser beating, respectively, for the following set of parameters: $n_q/n_0 = 0.1, eA_2/m\omega_p c = 0.9, \omega_1 a/c = 20$, $\omega_p a/c = 1.5, \omega_c a/c = 0.05$. The terahertz yield is significantly higher for TM_{10} mode laser beating than TE_{10} mode laser beating. Since terahertz wave has a TM_{10} polarization, a matched polarization is crucial for high output power. In Fig. 7 we show normalized density ripple vs normalized terahertz frequency for TM_{10} and TE_{10} mode laser beating. The frequency of THz radiation is decided by the difference in laser frequencies. For a given frequency difference the THz generation could be made a resonant process by a ripple of suitable wave number. This ripple wave number changes with the frequency of the THz wave. In Figs. 8 and 9 we plot normalized amplitude versus normalized cyclotron frequency curve for TM_{10} and TE_{10} mode laser beating, respectively. It shows that static transverse magnetic field increases the conversion efficiency.

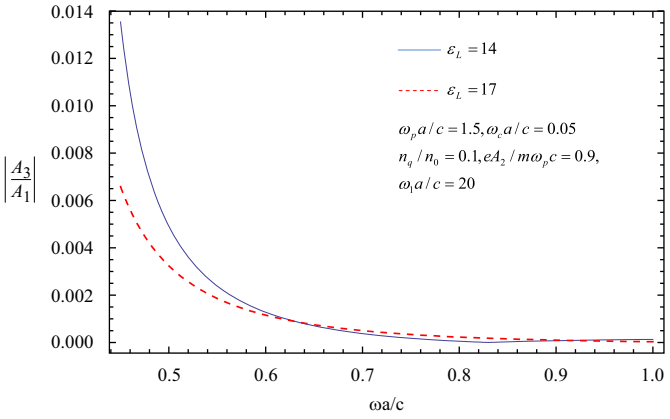

Fig. 5. Normalized amplitude versus normalized frequency curve of TM_{10} mode Terahertz radiation for TM_{10} mode laser beating for $\omega_p a/c = 1.5$, $\omega_c a/c = 0.05$, $n_q/n_0 = 0.1$, $eA_2/m\omega_p c = 0.9$, $\omega_1 a/c = 20$.

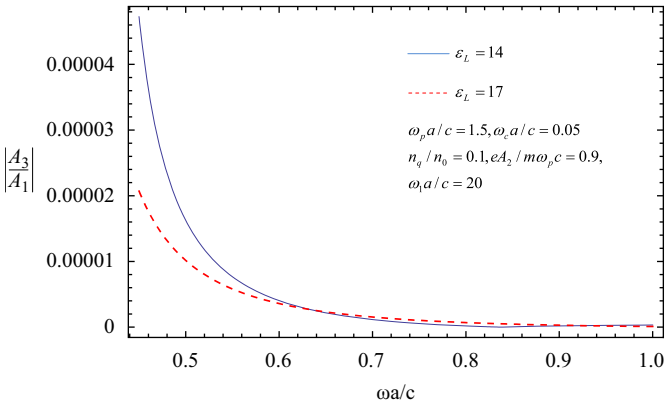

Fig. 6. Normalized amplitude versus normalized frequency curve of TM_{10} mode Terahertz radiation for TE_{10} mode laser beating for $\omega_p a/c = 1.5$, $\omega_c a/c = 0.05$, $n_q/n_0 = 0.1$, $eA_2/m\omega_p c = 0.9$, $\omega_1 a/c = 20$.

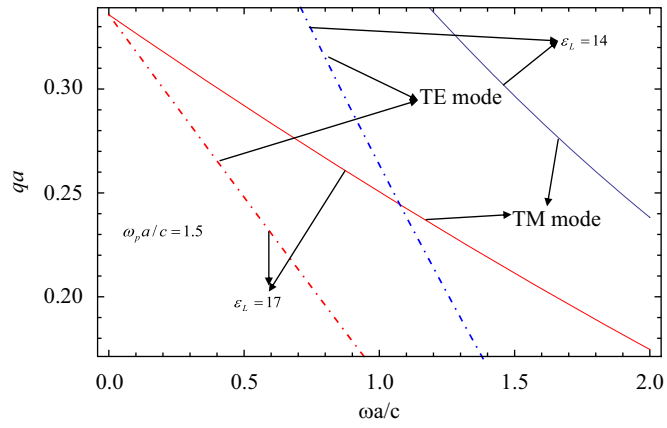

Fig. 7. Normalized density ripple versus normalized terahertz frequency curve.

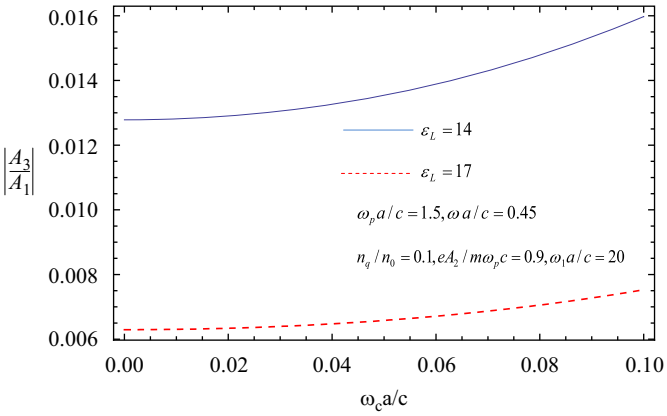

Fig. 8. Normalized amplitude versus normalized cyclotron frequency curve for TM_{10} mode laser beating for $\omega_p a/c = 1.5$, $\omega a/c = 0.45$, $n_q/n_0 = 0.1$, $eA_2/m\omega_p c = 0.9$, $\omega_1 a/c = 20$.

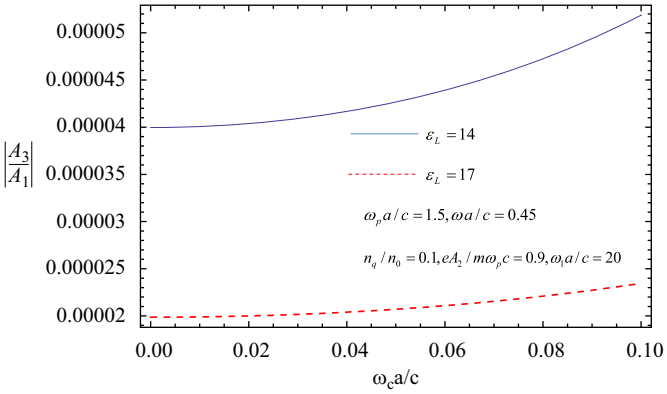

Fig. 9. Normalized amplitude versus normalized cyclotron frequency curve for TE_{10} mode laser beating for $\omega_p a/c = 1.5$, $\omega a/c = 0.45$, $n_q/n_0 = 0.1$, $eA_2/m\omega_p c = 0.9$, $\omega_1 a/c = 20$.

5. Discussion

In this paper we have examined terahertz generation at the beat frequency of two lasers inside a rippled semiconductor slab in the presence of transverse magnetic field. The terahertz amplitude is enhanced with magnetic field strength as observed in recent experiments [20]. Fig. 9 and (10) show normalized terahertz amplitude vs normalized cyclotron frequency curve for TM and TE mode laser beating, respectively. Also TM mode laser beating has higher yields of THz generation as compared to TE mode laser beating. The requisite phase matching is provided by the density ripple. The frequency of THz radiation is decided by the difference in laser frequencies. For a given frequency difference the THz generation could be made a resonant process by a ripple of suitable wave number. This ripple wave number changes with the frequency of the THz wave. For the parameters chosen in our calculations the normalized terahertz frequency varies in the range 0.45–1.0. At $\omega/2\pi = 1$ THz, the semiconductor slab could be of thickness 100 μm. The magnetic field strength required would be around 4 T.

The laser powers that we consider appropriate for THz generation in semiconductors correspond to oscillatory velocity to velocity of light in vacuum ratio $\sim e|E_1|/m\omega_1 c \approx e|E_2|/m\omega_2 c \approx .05$. For 10.6 μm CO_2 laser this requires an intensity of $\sim 2\times 10^{11} W/cm^2$.For pulse duration $\sim 1ps$ and spot size around a THz wavelength ($\approx 3\times 10^{-2} cm$), the requisite laser pulse energy turns out to be ~0.6 mJ. However, any change in carrier concentration at high laser intensity is not considered. Therefore we have not included transient photocurrent and surface effects. Also we have not included the effect of any damping mechanism in our calculations. The free electron collisions with phonons and impurities limit the growth. In case of thin sample surface scattering could also be significant.

Acknowledgment

One of the authors Manish Kumar is grateful to Institute of Technology, Banaras Hindu University for the financial support.

Appendix A

Consider a n-type semiconductor with free electron density n_0 immersed in a dc magnetic field $B_s\hat{y}$. It is subjected to an ac electric field, $\vec{E} = \vec{A}\, e^{-i(\omega t)}$. The electron response to this field is governed by the linearized equation of motion

$$m\frac{\partial \vec{v}}{\partial t} = -e\vec{E} - \frac{e}{c}\vec{v}\times\vec{B}_s \tag{1}$$

Replacing $\partial/\partial t$ by $-i\omega$ one obtains the drift velocity components

$$v_x = -\frac{e}{m(\omega^2-\omega_c^2)}[i\omega E_x + \omega_c E_z] \tag{2}$$

$$v_y = -\frac{ie}{m\omega}E_y \tag{3}$$

$$v_z = \frac{e}{m(\omega^2-\omega_c^2)}[-i\omega E_z + \omega_c E_x] \tag{4}$$

The current density $\vec{J} = -n_0 e\vec{v}$ thus has the following components:

$$J_x = \frac{n_0 e^2}{m(\omega^2-\omega_c^2)}[i\omega E_x + \omega_c E_z] \tag{5}$$

$$J_y = \frac{in_0 e^2}{m\omega}E_y \tag{6}$$

$$J_z = -\frac{n_0 e^2}{m(\omega^2-\omega_c^2)}[-i\omega E_z + \omega_c E_x] \tag{7}$$

Please cite this article as: M. Kumar, et al., J. Phys. Chem. Solids (2011), doi:10.1016/j.jpcs.2011.10.031

One may write $\vec{J} = \underline{\underline{\sigma}}.\vec{E}$ with the effective permittivity tensor is defined as

$$\underline{\underline{\varepsilon}} = \varepsilon_L + \frac{i4\pi}{\omega} \tag{9}$$

where

$$\underline{\underline{I}} = \begin{vmatrix} 1 & 0 & 0 \\ 0 & 1 & 0 \\ 0 & 0 & 1 \end{vmatrix}$$

is unit dyadic,

$$\varepsilon_{xx} = \varepsilon_{zz} = \varepsilon_L - \frac{\omega_p^2}{\omega^2 - \omega_c^2},$$

$$\varepsilon_{yy} = \varepsilon_L - \frac{\omega_p^2}{\omega^2}, \quad \varepsilon_{xz} = -\varepsilon_{zx} = -i\frac{\omega_c}{\omega}\frac{\omega_p^2}{\omega^2 - \omega_c^2},$$

References

[1] P.Y. Han, G.C. Cho, X.–C. Zhang, Opt. Lett. 25 (2000) 242–245.
[2] J.W. Waters, L. Froidevaux, R.S. Harwood, R.F. Jarnot, H.M. Pickett, W.G. Read, P.H. Siegel, R.E. Cofield, M.J. Filipiak, D.A. Flower, J.R. Holden, G.K. Lau, N.J. Livesey, G.L. Manney, H.C. Pumphrey, M.L. Santee, D.L. Wu, D.T. Cuddy, R.R. Lay, M.S. Loo, V.S. Perun, M.J. Schwartz, P.C. Stek, R.P. Thurstans, M.A. Boyles, K.M. Chandra, M.C. Chavez, G.-S. Chen, B.V. Chudasama, R. Dodge, R.A. Fuller, M.A. Girard, J.H. Jiang, Y. Jiang, B.W. Knosp, R.C. LaBelle, J.C. Lam, K.A. Lee, D. Miller, J.E. Oswald, N.C. Patel, D.M. Pukala, O. Quintero, D.M. Scaff, W.V. Snyder, M.C. Tope, P.A. Wagner, M.J. Walch, IEEE Trans. Geosci. Remot Sensing 44 (2006) 279–290.
[3] M. van Exter, D. Grischkowsky, IEEE Trans. Microwave Theory Tech. 38 (1990) 1684–1691.
[4] Y.C. Shen, T. Lo, P.F. Taday, B.E. Cole, W.R. Tribe, M.C. Kemp, Appl. Phys. Lett 86 (2005) 241116.
[5] M. Joffre, A. Bonvalet, A. Migus, J.-L. Martin, Opt. Lett. **21** (13) (1996) 964.
[6] W. Shi, Y.J. Ding, N. Fernelius, K. Vodopyanov, Opt. Lett. **27** (16) (2002) 1454–1456.
[7] K.H. Yang, P.L. Richards, Y.R. Shen, Appl. Phys. Lett. 19 (1971) 320.
[8] G. Balestrino, S. Martellucci, P.G. Medaglia, A. Paoletti, G. Petrocelli, A. Tebano, A. Tucciarone, F. Gelli, E. Giorgetti, S. Sottini, L. Tapfer, Appl. Phys. Lett. 78 (2001) 1204.
[9] W. Shi, Y.J. Ding, Appl. Phys. Lett. 84 (2004) 1635.
[10] K. Kawase, M. Sato, T. Taniuchi, H. Ito, Appl. Phys. Lett. **68** (1996) 2483.
[11] H. Hamster, A. Sullivan, S. Gordan, W. White, R.W. Falcone, Phys. Rev. Lett. 71 (1993) 2725.
[12] W.P. Leemans, et al., Phys. Rev. Lett. 91 (2003) 074802.
[13] G.L. Carr, M.C. Martin, W.R. McKinney, K. Jordan, G.R. Neil, G.P. Williams, Nature 420 (2002) 153.
[14] J. Yoshii, C.H. Lai, T. Katsouleasv, C. Joshi, W.B. Mori, Phys. Rev. Lett. 79 (1997) 4194.
[15] T.M.J. Antonsen, J. Palastro, H.M. Michberg, Phys. Plasmas 14 (2007) 033107.
[16] L. Bhasin, V.K. Tripathi, Phys. of Plasmas 16 (2009) 103105.
[17] M. Kumar, L. Bhasin, V.K. Tripathi, Phys. Scr. 81 (2010) 045504.
[18] D. Hashimshony, A. Zigler, K. Papadopoulos, Appl. Phys. Lett. 74 (12) (1999) 1669.
[19] Y.D. Glinka, D. Maryenko, J.H. Smet, Phys. Rev. B 78 (2008) 035328.
[20] R. McLaughlin, A. Corchia, M.B. Johnstan, Q. Chen, C.M. Ciesla, D.D. Arnone, G.A.C. Jones, E.H. Linfield, A.G. Davies, M. Pepper, Appl. Phys. Lett. 76 (2000) 2038.
[21] D.D. Arnone, C.M. Ciesla, A. Corchia, S. Egusa, M. Pepper, J.M. Chanberlain, C. Bezant, R. Clothier and N. Kharmmo, presentation at the EOS/SPIE International Symposia, 14–18 June 1999.
[22] S. Izumida, S. Ono, Z. Liu, H. Ohtake, N. Sarukura, J. Nonlinear Opt. Phys. Mater 8 (1999) 71.
[23] N. Sarukura, H. Ohtake, S. Izumuda, Z. Liu, J. Appl. Phys. 84 (1998) 654.
[24] S. Izumida, S. Ono, Z. Liu, H. Ohtake, N. Sarukura, Appl. Phys. Lett. 75 (1999) 451.
[25] J.N. Heyman, P. Neocleous, D. Hebert, P.A. Crowell, T. Muller, K. Unterrainer, Phys. Rev. B 64 (2001) 085202.
[27] A.Ya. Shulman, S.D. Ganichev, I.N. Kotelnikov, E.M. Dizhur, W. Prettl, A.B. Ormont, Yu.V. Fedorov, E. Zepezauer, phys. stat. sol. (a) 175 (1999) 289.

Please cite this article as: M. Kumar, et al., J. Phys. Chem. Solids (2011), doi:10.1016/j.jpcs.2011.10.031